Bistability in chemical reaction networks: Theory and application to the peroxidase–oxidase reaction

Baltazar D. Aguda and Bruce L. Clarke

Citation: The Journal of Chemical Physics **87**, 3461 (1987); doi: 10.1063/1.452991
View online: http://dx.doi.org/10.1063/1.452991
View Table of Contents: http://scitation.aip.org/content/aip/journal/jcp/87/6?ver=pdfcov
Published by the AIP Publishing

Bistability in chemical reaction networks: Theory and application to the peroxidase–oxidase reaction

Baltazar D. Aguda and Bruce L. Clarke
Department of Chemistry, University of Alberta, Edmonton, Alberta T6G 2G2, Canada

(Received 27 April 1987; accepted 2 June 1987)

Starting with a comprehensive list of elementary steps in the mechanism of the peroxidase–oxidase (PO) reaction, we extract the part of the mechanism essential to the experimentally observed bistability. A general systematic method is used to sort out the mechanism. First the extreme currents are found and the structure of the current polytope is determined. Then conditions for the existence of multiple steady states are used to identify the dominant extreme currents that are essential for bistability. A clue to the cause of bistability came from applying stoichiometric network analysis to the much simpler classical substrate-inhibition enzyme mechanism. Three extreme currents are essential for bistability. These correspond to (i) a reversible flux of the inhibiting substrate, (ii) the catalytic cycle, and (iii) an inhibition pathway coupled to the catalytic cycle. The same three elements are found in the PO mechanism. Analysis of the model containing these elements shows that bistability requires less ferriperoxidase than compounds I and II taken together. The PO model can exhibit damped oscillations simultaneously with bistability, simulate experimentally observed phases in the kinetics of the closed system, and demonstrate that enzyme inhibition by the substrate oxygen exists.

I. INTRODUCTION

The aerobic oxidation of NADH (nicotinamide adenine dinucleotide) catalyzed by the enzyme horseradish peroxidase [Eq. (1.1)], here referred to as the peroxidase–oxidase (PO) reaction, is known to exhibit damped and sustained oscillations, bistability, and even chaos in an open system[1]:

$$2\mathrm{NADH} + 2\mathrm{H}^+ + \mathrm{O}_2 \rightarrow 2\mathrm{NAD}^+ + 2\mathrm{H}_2\mathrm{O}. \qquad (1.1)$$

Simple models to account for these observed behaviors have been proposed before. Degn and Mayer[2] investigated two-species models derived from the old Lotka model[3] to simulate damped oscillations while Olsen and Degn[1,4] concocted a four-species model based on the main features of the complex mechanism and successfully reproduced the qualitative forms of the sustained oscillations. Recently, Olsen[5,6] has developed a four-species model that shows chaos for some enzyme concentrations. No model has yet been developed for the bistable behavior, although it has been suggested that bistability is probably caused by the inhibition of the enzyme due to high oxygen concentrations as supported experimentally by Degn, Olsen, and Perram.[1] It has been known for a long time[7] that substrate inhibition is one of the possible mechanisms that lead to bistability in an open system.

Sufficient information is now known about the mechanistic details of the PO reaction that computer simulations of the closed system sometimes agree with experimental data almost quantitatively.[8,9] Eventually, quantitative models of the richer dynamics in the open system should be developed as well.

Different dynamical behaviors usually occur under different sets of conditions. The modeling can therefore be simplified by considering each dynamic behavior separately. In this paper we focus on bistability. Our purpose is to propose a systematic approach to modeling bistability not only in the PO reaction but in all complex reaction networks in general that are capable of having multiple steady states. As in the PO reaction, the list of elementary steps in the mechanism is often a long one and one wants to determine a minimal reaction subset, a "model," that is sufficient to generate bistability. The first important step in the approach is to identify the elementary steady state reaction pathways that comprise the reaction network at steady state. In the language of *Stoichiometric Network Analysis*,[10] any steady state of a reaction network is a superposition of a finite number of *extreme currents*. The second step requires a consideration of the "topology" of the network, i.e., how one extreme current is coupled to another and the reactions involved. This is accomplished by determining the structure of the *current polytope* Π_v, whose vertices represent the extreme currents. The third step is to devise a test that identifies the dominant extreme currents occurring under conditions where there are multiple steady states. The reactions in the dominant extreme currents compose the minimal model. Reactions that belong exclusively to the insignificant extreme currents are thrown away and considered as inessential.

Section II gives a summary of the formalism employed in *Stoichiometric Network Analysis* and Sec. III discusses criteria essential for the existence of multiple steady states. These criteria along with the structure of the current polytope are the key elements in our modeling approach. Section IV gives an illustration of the method applied to the reversible classical substrate-inhibition mechanism. What we learn from the analysis of this simpler mechanism provides guidance for the analysis of the complex PO mechanism. The modeling of the PO reaction, as well as an analysis of the model, is then treated extensively in Sec. V.

 0021-9606/87/183461-10$02.10

II. NETWORK TOPOLOGY AND THE CURRENT POLYTOPE

Let there be r one-way chemical reactions $R_1,...,R_r$ involving n species $X_1,...,X_n$. Let us also represent reversible reactions as two one-way reactions. Define an $n \times r$ matrix ν called the *stoichiometric matrix* whose element ν_{ij} is equal to the stoichiometric coefficient of X_i on the right-hand side of reaction R_j minus that on the left. If $\mathbf{X}$ is a vector of concentrations and $\mathbf{v}$ is a vector of one-way reaction rates, then the kinetic equations take the form

$$\dot{\mathbf{X}} = \nu \mathbf{v}(\mathbf{X},\mathbf{k}), \tag{2.1}$$

where $\dot{} = d/dt$, $\mathbf{k}$ is a vector of the rate constants, and $\mathbf{v}(\mathbf{X},\mathbf{k})$ means that the components of $\mathbf{v}$ are functions of the components of $\mathbf{X}$ and $\mathbf{k}$. In general, there are conservation conditions arising from the conservation of atoms or other subunits. Let there be d independent species taken as the first d species $X_1,...X_d$ without loss of generality. There are then $(n-d)$ conservation constraints and we can define a $(n-d) \times n$ *conservation matrix* γ by

$$\gamma \mathbf{X} = \mathbf{C},$$

where $\mathbf{C}$ is a vector with $(n-d)$ positive components. Let us assume mass action kinetics which give $\mathbf{v}$ the form

$$\mathbf{v} = (\text{diag } \mathbf{k})\mathbf{X}^{\kappa},$$

where $(\text{diag } \mathbf{k})$ is a $r \times r$ diagonal matrix with $\mathbf{k}$ along its diagonal and κ is the $n \times r$ *kinetic matrix* whose element κ_{ij} is the order of X_i in reaction R_j. The r-component vector $\mathbf{X}^{\kappa}$ has a jth component defined by

$$(\mathbf{X}^{\kappa})_j = \prod_{i=1}^{n} X_i^{\kappa_{ij}}$$

which is just the expression for the jth component of $\mathbf{v}$ without the rate constant. Equation (2.1) is thus written as

$$\dot{\mathbf{X}} = \nu(\text{diag } \mathbf{k})\mathbf{X}^{\kappa}. \tag{2.2}$$

Let $\mathbf{X}^0$ be a positive steady state of the network (all components are positive) satisfying the steady state equation

$$\nu \mathbf{v}^0(\mathbf{X}^0,\mathbf{k}) = \mathbf{0}. \tag{2.3}$$

We now present the form of Eq. (2.2) that is used in stoichiometric analysis.[10,11] The dynamical variables are the scaled concentrations x_i defined by

$$x_i = X_i/X_i^0$$

or in matrix form:

$$\mathbf{x} = (\text{diag } \mathbf{1}/\mathbf{X}^0)\mathbf{X}.$$

The nonlinear equations of motion now become

$$\dot{\mathbf{x}} = (\text{diag } \mathbf{1}/\mathbf{X}^0)\nu(\text{diag } \mathbf{v}^0)\mathbf{x}^{\kappa}, \tag{2.4}$$

where $\mathbf{v}^0$ is a steady state rate vector satisfying Eq. (2.3) and which is referred to as a *current*. Note that in particular, a steady state solution to Eq. (2.4) is $\mathbf{x}^0 = \mathbf{e} = (1,1,...,1)^t$ (t = transpose). At this point, we introduce one of the parameters of stoichiometric network analysis, $\mathbf{h} \in R^n_+$, defined by

$$\mathbf{h} = \mathbf{1}/\mathbf{X}^0 = (1/X_1^0,...,1/X_n^0).$$

Because of the constraint of stoichiometry on the dynamics of chemical reactions, we are not free to use any $\mathbf{v}^0$ in the nonnegative orthant of r-dimensional Euclidean space, R^r_+. In other words, $\mathbf{v}^0$ cannot be an arbitrary parameter. From Eq. (2.3), we see that all solutions $\mathbf{v}^0$ must lie in a $(r-d)$-dimensional space S_v which is orthogonal to the d-dimensional space S_d spanned by the d independent row vectors of ν. Since all the components of $\mathbf{v}^0$ are nonnegative, $\mathbf{v}^0$ must lie in the intersection of S_v and R^r_+. This intersection is a convex polyhedral cone called the *current cone* and denoted as $\mathscr{C}_v$. Let there be f edge vectors supporting the cone's frame and whose directions are given by $\mathbf{E}^1,...,\mathbf{E}^f$. Then every $\mathbf{v}^0 \in \mathscr{C}_v$ can be expressed as a nonnegative linear combination of these $\mathbf{E}^i$'s:

$$\mathbf{v}^0 = \sum_{i=1}^{f} j_i \mathbf{E}^i$$

or in matrix form:

$$\mathbf{v}^0 = \mathbf{E}\mathbf{j}, \tag{2.5}$$

where the $r \times f$ matrix $\mathbf{E}$ is called the *current matrix* and $\mathbf{j}$ is the current parameter $\mathbf{j} \in R^f_+$. The matrix $\mathbf{E}$ is found from ν. An APL algorithm called CURRENTS which finds $\mathbf{E}$ from a given ν is provided in Ref. 11. The columns of $\mathbf{E}$ give the set of *extreme currents* for the given network. The example given in Sec. IV will make this interpretation clearer.

The manifold of steady states $\mathscr{M}$, whose dimension is $(n-d)+r$, is now parametrized by the convex parameters $(\mathbf{h},\mathbf{j})$:

$$\mathscr{M} = \{(\mathbf{h},\mathbf{v}^0(\mathbf{j})) \in R^n_+ \times \mathscr{C}_v\},$$
$$\mathscr{C}_v = \{\mathbf{v}^0 | \mathbf{v}^0 = \mathbf{E}\mathbf{j}, \mathbf{j} \in R^f_+\}.$$

Note that motion along a ray $\mathbf{j} \in \mathscr{C}_v$ (e.g., $\lambda \mathbf{j}$, $\lambda > 0$) is equivalent to multiplying simultaneously (by the same amount) all the rate constants (i.e., $\lambda \mathbf{k}$) of all the reactions involved in the current. As is obvious from Eq. (2.2), this operation does not affect the value of $\mathbf{X}^0$. This means that $\mathbf{h}$ and $\mathbf{j}$ can be assigned values independently. It is clear that any cross section of $\mathscr{C}_v$ contains all the information available from the current cone. This $(r-d-1)$-dimensional cross section is called the *current polytope* Π_v defined as

$$\Pi_v = \{\mathbf{v}^0 | \mathbf{v}^0 = \mathbf{E}\mathbf{j},\ \mathbf{e}'\mathbf{v}^0 = 1\}.$$

The vertices of Π_v correspond to the extreme currents. The structure of Π_v, i.e., the adjacency relation among the vertices, the edges, 2-faces up to $(r-d-2)$-faces can be determined using already existing APL programs due to von Hohenbalken.[12]

The structure of Π_v is useful in the following way. When one reaction listed in the mechanism is known experimentally to be slow compared to the other reactions, then the extreme currents involving this reaction must have a small contribution to the steady state. The point inside Π_v corresponding to the steady state parameter $\mathbf{j}$ must be far from the vertices corresponding to those extreme currents. The dominant extreme currents are those represented by the remaining vertices. These extreme currents consist entirely of reactions that are relatively fast at steady state. Two distant extreme currents or vertices of Π_v cannot be both important under the same conditions. Thus Π_v contains topological

information that forces us to make an either–or decision about the importance of sets of reactions.

Stoichiometric relationships among major reactants and products are often known experimentally. Sometimes several different possible stoichiometries for the overall reaction are consistent with the mechanism. These stoichiometries are associated directly with different parts of Π_v. Thus experimental information about the overall stoichiometry can also help locate the dominant extreme currents, or equivalently, the dominant vertices of Π_v.

Next, we show that there is an inner structure of Π_v that indicates whether the reaction network is capable of multiple steady states or not.

III. CRITERIA FOR THE EXISTENCE OF MULTIPLE STEADY STATES

A network with more than one isolated steady state must have a steady state manifold $\mathcal{M}$ that folds back at some feasible values of $(\mathbf{C},\mathbf{k})$. These fold points of $\mathcal{M}$ are singular points and they are characterized by the vanishing of the corresponding Jacobian of the set of independent kinetic equations. If we divide the matrices and vectors into independent and dependent components as follows:

$$\mathbf{h}=\begin{pmatrix}\mathbf{h}_I\\ \mathbf{h}_D\end{pmatrix},\quad \boldsymbol{\nu}=\begin{pmatrix}\boldsymbol{\nu}_I\\ \boldsymbol{\nu}_D\end{pmatrix},$$

$$\boldsymbol{\kappa}=\begin{pmatrix}\boldsymbol{\kappa}_I\\ \boldsymbol{\kappa}_D\end{pmatrix},\quad \boldsymbol{\gamma}=(\boldsymbol{\gamma}_I,\boldsymbol{\gamma}_D);$$

the Jacobian matrix has the expression

$$\frac{\partial \dot{\mathbf{x}}_I}{\partial \mathbf{x}_I}=(\operatorname{diag}\mathbf{h}_I)\boldsymbol{\nu}(\operatorname{diag}\mathbf{Ej})(\boldsymbol{\kappa}_g)^t, \tag{3.1}$$

where the generalized kinetic matrix $\boldsymbol{\kappa}_g$ is defined by

$$(\boldsymbol{\kappa}_g)^t=(\boldsymbol{\kappa}_I)^t+(\boldsymbol{\kappa}_D)^t\left(\frac{\partial \mathbf{x}_D}{\partial \mathbf{x}_I}\right),$$

$$\left(\frac{\partial \mathbf{x}_D}{\partial \mathbf{x}_I}\right)=-(\operatorname{diag}\mathbf{h}_D)(\boldsymbol{\gamma}_D)^{-1}\boldsymbol{\gamma}_I(\operatorname{diag}\mathbf{h}_I)^{-1}.$$

Note that $(\boldsymbol{\gamma}_D)^{-1}$ must exist, otherwise the concentrations of the dependent species cannot be solved in terms of the independent ones.

If we write the characteristic equation as

$$P(\lambda)=\sum_{i=0}^{d}\alpha_i\lambda^{d-i}=0$$

then we see that

$$\alpha_d=(-1)^d\det\left(\frac{\partial \dot{\mathbf{x}}_I}{\partial \mathbf{x}_I}\right).$$

In other words, a necessary test for the existence of multiple steady states is the existence of some $(\mathbf{h},\mathbf{j})$ such that

$$\alpha_d(\mathbf{h},\mathbf{j})=0 \tag{3.2}$$

which results to one vanishing eigenvalue. Equation (3.2) says that if α_d is positive for all sets of steady state parameters then no multiplicity of steady states is possible.

We now develop an additional criterion which turns out to be very helpful in the PO model. Our criterion is that an experimental system with bistability lies on a two-dimensional face of Π_v and that this face will contain part of the surface defined by Eq. (3.2). The reasons for this will be developed in the discussion which follows.

Equation (3.2) is an equation of a hypersurface Σ^0 which can be drawn inside Π_v for a given $\mathbf{h}$. If $\boldsymbol{\gamma}=\varnothing$ then Σ^0 has a fixed position in Π_v regardless of the value of the parameter $\mathbf{h}$. An example of this has already been given by Clarke (Ref. 10, p. 38) for the one-dimensional Schlogl model. However, if there are conservation conditions, then the position of Σ^0 will depend on the value of $\mathbf{h}$. In either case, this hypersurface must exist if there is the possibility of multiple steady states at all.

The sign of α_d is related to stability. In a bistable system, there is a middle unstable steady state that corresponds to the region in Π_v where α_d is negative and two stable steady states that correspond to nearby regions where α_d is positive. Thus, the parameters of an experimental bistable system must place the system in the vicinity of the hypersurface Σ^0.

Another important ingredient is the following principle:

Principle of simplicity: *An experimental system will probably correspond to the lowest dimensional face of* Π_v *that is consistent with the observed experimental behavior.*

The reasoning behind this principle involves the fact that chemical reaction rates vary over many orders of magnitude. Usually the rates of the less important reactions in chemical system at steady state are many orders of magnitude smaller than the rates of the dominant reactions. It would be improbable for a large number of independent currents to be equal at steady state. Thus the center of Π_v is the least probable location to find an experimental system because in this region all currents are equal. Π_v has faces that are one lower dimension than the polytope itself. The centers of these faces are also improbable because all but one current in a set of independent currents must be equal. The most probable locations for finding an experimental system are near the lowest dimensional faces, with vertices having the highest probability of all.

We now consider the lowest dimensional face of Π_v that is consistent with bistability. A vertex is unacceptable. It represents an extreme current where the reaction rates are locked into fixed ratios. To have several steady states at a vertex, the only thing that can vary is the flow in this single current. Mathematically several steady states are possible only if the reaction kinetics is of high order, however, it seems unlikely that any realistic chemical network would meet the required mathematical conditions. Our view of bistability is that the three steady states (two stable, one unstable) differ in that each state has a different combination of important reactions. Thus there should be three independent combinations of reactions involved. Three independent currents span a three-dimensional cone, which corresponds to a two-dimensional subset of Π_v. These three currents are unlikely to lie on opposite sides of Π_v because this would violate the principle of simplicity. Therefore, they should lie on a two-dimensional face of Π_v. In order to have bistability on this face, the curve Σ^0 must also pass through the interior of the face. Thus, in our search for a model for the PO reaction's bistability, we begin by looking at the 2-faces of Π_v.

IV. ELEMENTS IN THE SUBSTRATE-INHIBITION MECHANISM ESSENTIAL FOR BISTABILITY

In this section, we illustrate the method of stoichiometric network analysis on the reversible classical substrate-inhibition enzyme mechanism and show explicitly how the modeling approach works. From this example, we shall list the essential elements in the mechanism that are responsible for the bistability and will serve as our guide in the analysis of the PO reaction mechanism.

The list of reactions is given below. Reactions (R1) and (R2) represent the reversible flux of the substrate S from a constant reservoir denoted by ( ). E represents the free enzyme, ES and SES are enzyme–substrate complexes. The symbol (P) means a constant product reservoir:

$$(\ ) \rightarrow S, \tag{R1}$$

$$S \rightarrow (\ ), \tag{R2}$$

$$S + E \rightarrow ES, \tag{R3}$$

$$ES \rightarrow E + (P), \tag{R4}$$

$$S + ES \rightarrow SES, \tag{R5}$$

$$SES \rightarrow S + ES, \tag{R6}$$

$$ES \rightarrow S + E, \tag{R7}$$

$$E + (P) \rightarrow ES. \tag{R8}$$

The current matrix **E** is

$$\mathbf{E} = \begin{pmatrix} 1 & 1 & 0 & 0 & 0 & 0 \\ 1 & 0 & 0 & 0 & 0 & 1 \\ 0 & 1 & 0 & 1 & 0 & 0 \\ 0 & 1 & 0 & 0 & 1 & 0 \\ 0 & 0 & 1 & 0 & 0 & 0 \\ 0 & 0 & 1 & 0 & 0 & 0 \\ 0 & 0 & 0 & 1 & 0 & 1 \\ 0 & 0 & 0 & 0 & 1 & 1 \end{pmatrix}$$

and the six extreme current diagrams are shown in Fig. 1. Note that the nonzero entries correspond to the reactions comprising the extreme currents corresponding to the columns. Π_v is four-dimensional and there are 14 edges, 15 2-faces, and 7 3-faces. Table I lists all the 2-faces in terms of the component extreme currents (column numbers of **E**). The signs of the terms in α_d for each face are also given.

TABLE I. Two-dimensional faces of Π_v and signs of the terms in α_d. (Numbers in the first column give the column numbers of the current matrix **E**; n = number of species in each 2-face; d = number of independent species.)

2-face	n	d	α_d
1 2 3	4	3	+ −
1 2 4	3	2	+
1 2 5	3	2	+
1 3 4	4	3	+
1 3 5	4	3	+
1 3 6	4	3	+
1 4 6	3	2	+
1 5 6	3	2	+
2 3 4	4	3	+ −
2 3 5	4	3	+ −
2 4 5	3	2	+
3 4 5	4	3	+
3 4 6	4	3	+
3 5 6	4	3	+
4 5 6	3	2	+

There are only three possible 2-faces that can have terms of both signs so that their α_d's vanish for some parameters $(\mathbf{h},\mathbf{j})$. It can be shown that the 2-faces (2 3 4) and (2 3 5) can have either two or zero steady states for all parameters. Only the face (1 2 3) can generate three steady states. Thus, we can take reactions (R1)–(R6) as the minimal reaction set for a bistable model. Reactions (R7) and (R8) do not occur in this facet of Π_v and are therefore inessential.

The current polytope for the bistable model is given in Fig. 2. The $\{\alpha_d = 0\}$ curve is also given for a fixed $\mathbf{h} = (1/E^\circ, 1/S^\circ, 1/ES^\circ, 1/SES^\circ)^t$. The vanishing of α_d occurs when

$$j_1(h_1h_3 + h_1h_4 + h_3h_4) + j_2h_3(h_4 - h_1) = 0 \tag{4.1}$$

or using the conservation condition for the total enzyme concentration E_t:

$$j_1/j_2 = (h_4^{-1} - h_1^{-1})/E_t \tag{4.2}$$

from which we conclude that multiplicity of steady states occurs when $[SES]^\circ > [E]^\circ$. Since the steady states of these species can be determined experimentally, this kind of conclusion is quite amenable to verification.

The steady state manifold for this minimal model possesses a degenerate singularity which is the cusp. In fact, from an analysis of the cust catastrophe manifold,[13] we can exactly express the set of parameters that lead to three dis-

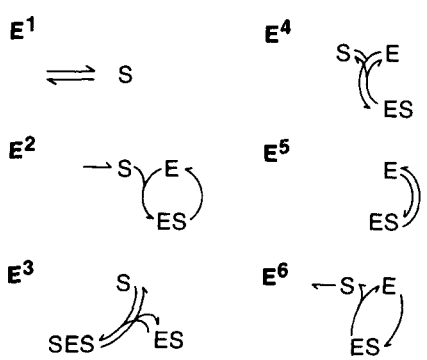

FIG. 1. The six extreme currents corresponding to the columns of the current matrix **E** for the reversible classical substrate-inhibition enzyme mechanism.

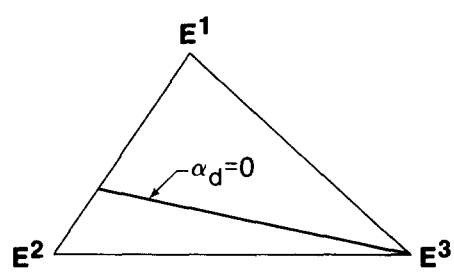

FIG. 2. The current polytope Π_v of the reduced substrate-inhibition mechanism involving currents $\mathbf{E}^1$, $\mathbf{E}^2$, $\mathbf{E}^3$ given in Fig. 1. For a fixed parameter **h**, $\alpha_d = 0$ is a straight line as shown.

tinct steady states. We define the *tristate set* T as the set of parameters $(E_t,\mathbf{k})$ that induce three positive steady states. T for the minimal model is

$$\mathbf{T}=\{(\beta_2,\beta_1,\beta_0)\,|\,\beta_2<0,\ \beta_1>0,\ \beta_0<0,\ \text{and}\quad K<0\},\tag{4.3}$$

where

$$K=27\beta_0^2+4\beta_0\beta_2^3-18\beta_0\beta_1\beta_2-\beta_1^2\beta_2^2+4\beta_1^3,$$
$$\beta_0=-k_1k_4k_6/k_2k_3k_5,$$
$$\beta_1=(k_4k_6/k_3k_5)+(k_4k_6E_t/k_2k_5)-(k_1k_6/k_2k_5),$$
$$\beta_2=(k_6/k_5)-(k_1/k_2).$$

The analysis above tells us that $\mathbf{E}^2$, the pathway corresponding to the catalytic cycle, and $\mathbf{E}^3$ which is the enzyme inhibition pathway, are sufficient to generate a fold on $\mathcal{M}$. For bistability or three steady states, $\mathcal{M}$ must fold twice and $\mathbf{E}^1$, the reversible flux of substrate, is a necessary addition. The three elements $\mathbf{E}^1$, $\mathbf{E}^2$, and $\mathbf{E}^3$ in this minimal model will have their counterparts in the bistable model for the PO reaction.

V. A BISTABLE MODEL FOR THE PO REACTION

A. The model

We start with all the reactions that have been studied or postulated previously for the PO reaction. The list is given in Table II. In particular, most of these reactions are from the table given by Olsen and Degn[4] and some are from Yokota and Yamazaki.[8]

We consider the case where NADH is in excess and assume a constant acidic *p*H. Hence, the concentrations of NADH, NAD^+, H^+ are not dynamical variables (i.e., they are assumed constant). For convenience, the following symbols for the dynamical species are used:

Enzymic species:

V: ferrousperoxidase;
W: ferriperoxidase;
X: compound I;
Y: compound II;
Z: compound III.

Nonenzymic species:

A: H_2O_2;
B: $NAD^{\cdot}$;
C: O_2^-;
F: O_2.

There are 17 extreme currents found from all the reactions listed in Table II. These are coded in the current matrix given below:

$$\mathbf{E}=\begin{pmatrix}
0&0&0&1&0&0&1&0&1&0&0&0&0&0&0&0&0\\
1&1&0&1&1&1&0&1&1&1&0&1&0&1&1&0&1\\
1&1&0&1&1&0&1&1&1&0&1&1&1&1&0&0&0\\
0&0&0&0&0&1&0&0&0&1&0&0&0&0&1&1&1\\
1&2&0&0&0&0&0&1&0&1&1&1&0&0&0&0&0\\
1&1&0&0&0&0&0&0&0&0&1&1&0&0&0&0&0\\
0&0&0&0&0&0&0&0&0&0&1&1&1&1&1&1&1\\
1&0&0&0&1&1&0&0&0&0&0&0&0&0&0&0&0\\
0&0&0&0&0&0&1&0&0&0&1&0&1&0&0&1&0\\
0&0&0&0&1&0&0&1&0&0&0&0&1&1&0&0&0\\
0&0&0&2&1&1&2&1&1&1&1&0&2&1&2&2&1\\
0&0&0&0&0&1&1&0&1&1&0&0&0&0&0&1&1\\
0&0&0&0&0&0&0&0&1&0&0&1&0&1&0&0&1\\
0&0&0&1&0&0&0&0&0&0&0&0&0&0&1&0&0\\
0&1&0&0&0&0&0&1&0&1&0&0&0&0&0&0&0\\
1&1&1&1&1&1&1&1&1&1&1&1&1&1&1&1&1\\
0&0&1&0&0&0&0&0&0&0&0&0&0&0&0&0&0
\end{pmatrix}.$$

Figure 3 shows the extreme currents represented by columns 3, 5, 9, and 14 of E which we will see later to be important.

The dimension of Π_v is 8 and there are 90 edges, 233 2-faces, 346 3-faces, 315 4-faces, 179 5-faces, 62 6-faces, and 12 7-faces. We now identify all the possible extreme currents that fall under each of the three elements responsible for the bistability in the example analyzed in Sec. IV. Current $\mathbf{E}^3$ represents the reversible flux of the inhibiting substrate O_2. The classical peroxidase catalytic cycle is given by only one extreme current, namely $\mathbf{E}^9$.

There are several choices for the inhibition pathway. Each should involve the formation and decay of the inactive enzyme intermediate compound III (*Z*). According to Yamazaki and Piette,[14] the reaction between the superoxide anion radical O_2^- (*C*) and ferriperoxidase (*W*) appears to be

TABLE II. Elementary processes in the peroxidase–oxidase mechanism.

R_1	$Per^{3+} + H_2O_2$	→	Co I
R_2	Co I + NADH	→	Co II + NAD·
R_3	Co II + NADH	→	Per^{3+} + NAD·
R_4	Co II + H_2O_2	→	Co III
R_5	Per^{3+} + NAD·	→	Per^{2+} + NAD^+
R_6	$Per^{2+} + O_2$	→	Co III
R_7	Co III + NADH	→	Co I + NAD· + H^+
R_8	Co III + NAD·	→	Co I + NAD^+
R_9	Co I + O_2^-	→	Co II + O_2
R_{10}	$Per^{3+} + O_2^-$	→	Co III
R_{11}	NAD· + O_2	→	$NAD^+ + O_2^-$
R_{12}	$H^+ + O_2^- +$ NADH	→	H_2O_2 + NAD·
R_{13}	2NAD· + H^+	→	NADH + NAD^+
R_{14}	$2O_2^- + 2H^+$	→	$H_2O_2 + O_2$
R_{15}	Per^{2+} + Co III	→	Per^{3+} + Co I
R_{16}		→	O_2
R_{17}	O_2	→	

the most likely path of compound III formation. This information leads us to consider $\mathbf{E}^5$, $\mathbf{E}^8$, $\mathbf{E}^{13}$, and $\mathbf{E}^{14}$. Among these, the most likely choice is $\mathbf{E}^5$. Reaction R_7 (of Table II) is known to be very slow[15–17] and it is suggested by Yokota and Yamazaki[8] and others[18] that reaction R_8 (of Table II) explains the characteristic compound III decay.

When we look at the faces of Π_v, we discover that (3 5 9), (3 9 14), and (3 8 9) are 2-faces. It can be shown that neither (3 9 14) nor (3 8 9) can give rise to a bistable model. A model based on (3 9 14) will always have a unique steady state for every set of parameters while (3 8 9) can only have at most 2 steady states for any set of parameters. Indeed, a model based on (3 5 9) can exhibit bistability for some parameter values. This is our proposed model and we give the network diagram in Fig. 4.

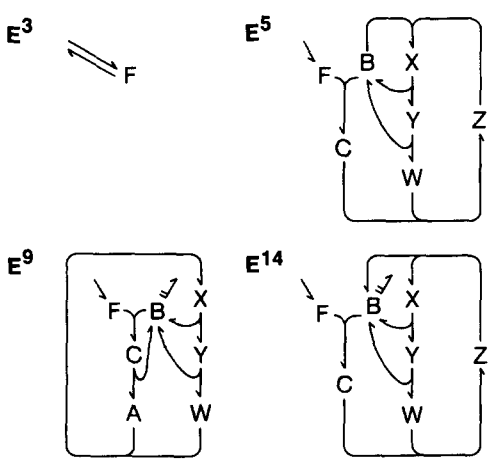

FIG. 3. Four important extreme currents found in the peroxidase–oxidase mechanism given in Table II. $\mathbf{E}^3$ corresponds to the reversible flux of the substrate oxygen (F), $\mathbf{E}^9$ is the classical peroxidase catalytic cycle, and the two extreme currents $\mathbf{E}^5$ and $\mathbf{E}^{14}$ are possible enzyme inhibition pathways involving the inactive intermediate compound III (Z).

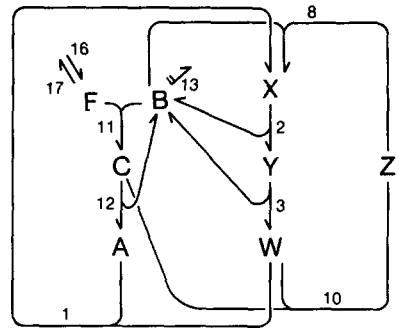

FIG. 4. Network diagram of the bistable model for the peroxidase–oxidase reaction. Reaction numbers refer to those given in Table II. Every steady state of this model is a linear combination of the extreme currents $\mathbf{E}^3$, $\mathbf{E}^5$, and $\mathbf{E}^9$ shown in Fig. 3.

We notice that this model closely resembles the one proposed by Fed'kina *et al.*[18] for the sustained oscillations exhibited by the PO reaction. However, their model lacks, reaction R_{17} (of Table II) and assumes a linear termination reaction, R_{13} (of Table II). Because their model leads to only two extreme currents, bistability is not possible.

B. Bistability and damped oscillations

It was determined that $\alpha_d = 0$ for the model if and only if

$$h_8^{-1}[j_3 j_9 + (j_5 + 2j_9)(j_5 + j_9)] + h_5^{-1}(j_3 + 2j_5 + 2j_9)(j_5 + j_9) = (h_6^{-1} + h_7^{-1}) j_3 j_5$$

[note: $\mathbf{h}^{-1} = (A^0, B^0, C^0, F^0, W^0, X^0, Y^0, Z^0)^t$]

from which we find the following exact criterion for the existence of an $\{\alpha_d = 0\}$ curve in the interior of Π_v:

$$j_9/j_5 < (h_6^{-1} + h_7^{-1} - h_5^{-1})/(h_5^{-1} + h_8^{-1}), \quad (5.1)$$

which in turn requires that

$$h_5^{-1} < h_6^{-1} + h_7^{-1}. \quad (5.2)$$

In other words, if the conditions are such that the steady state concentration of ferriperoxidase is greater than the combined steady state concentrations of compounds I and II, then no bistability can occur. Π_v for the model is given in Fig. 5 with the $\{\alpha_d = 0\}$ curve for a fixed $\mathbf{h}$.

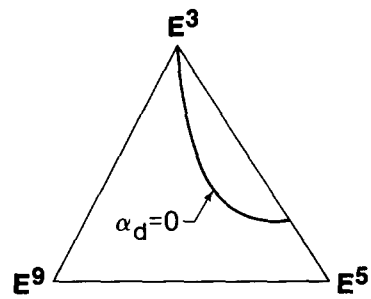

FIG. 5. The current polytope Π_v and a curve $\alpha_d = 0$ (for a fixed parameter $\mathbf{h}$) of the bistable model network given in Fig. 4.

The problem of solving the steady states, Eq. (2.3), for the model can actually be turned into a one-variable problem as will now be shown. Equation (2.5) gives the following relationship among the steady state velocities:

$$v_1^0 = v_{12}^0 = v_{13}^0,$$
$$v_2^0 = v_3^0 = v_{11}^0,$$
$$v_8^0 = v_{10}^0,$$
$$v_{16}^0 = v_{11}^0 + v_{17}^0,$$
$$v_{11}^0 = v_{12}^0 + v_{10}^0,$$

where the reaction velocities are

$$v_{16} = k_{16},$$
$$v_{17} = k_{17}F,$$
$$v_{11} = k_{11}FB,$$
$$v_{12} = k_{12}C,$$
$$v_1 = k_1AW,$$
$$v_2 = k_2X,$$
$$v_3 = k_3Y,$$
$$v_{10} = k_{10}CW,$$
$$v_8 = k_8BZ,$$
$$v_{13} = k_{13}B^2.$$

There is one conservation condition corresponding to that of the total enzyme concentration

$$E_t = W + X + Y + Z.$$

One can then express the steady states of seven of the eight species in terms of the remaining one. This last species is taken to be species B for convenience. Unless otherwise stated, the species symbols will also be taken as their steady state concentrations below. To determine the steady states, one first solves a cubic polynomial for the steady state value B:

$$f_3(B) = B^3 + \beta_2 B^2 + \beta_1 B + \beta_0 = 0, \tag{5.3}$$

where

$$\beta_0 = -k_8k_{16}k_{12}/k_{13}^2k_{10},$$
$$\beta_1 = (E_t + k_{12}/k_{10})(k_8k_{17}/k_{13}k_{11}) - (k_{16}/k_{13}),$$
$$\beta_2 = (E_t + k_{12}/k_{10})(k_8/k_{13}) + (k_{17}/k_{11}) - (1/k_3 + 1/k_2)(k_{16}k_8/k_{13}).$$

Not all positive real roots of Eq. (5.3) are allowed as steady state value for B. In order that all other species will have positive steady states, B must be less than a certain upper bound B_m:

$$B < B_m = [(k_{17}/2k_{11})^2 + (k_{16}/k_{13})]^{1/2} - (k_{17}/2k_{11}). \tag{5.4}$$

This is a consequence of the condition that W and Z must be positive as is obvious below. The steady states of all other species in terms of B are given by the following equations:

$$C = k_{13}B^2/k_{12},$$
$$F = k_{16}/(k_{17} + k_{11}B),$$
$$X = k_{11}BF/k_2,$$
$$Y = k_{11}BF/k_3,$$
$$W = (k_{11}BF/k_{10}C) - (k_{12}/k_{10}),$$
$$A = k_{13}B^2/k_1W,$$
$$Z = k_{10}k_{13}BW/k_8k_{12}.$$

Our previous results[13] on the analysis of the cusp catastrophe manifold enable us to define exactly the set of parameters that will give three positive steady states for the model. The tristate set **T** is given by Eq. (4.3) with the β coefficients given in Eq. (5.3). Furthermore, due to condition (5.4), there are other constraints on the parameters belonging to **T**, namely,

$$\{3B_m + \beta_2 > 0 \text{ and } f_3(B_m) > 0\}.$$

For the sake of demonstration, we provide the following parameter values that give three steady states:

$$k_{11} = 1\times10^8\ \mathrm{M^{-1}\,s^{-1}},$$
$$k_1 = 1\times10^7\ \mathrm{M^{-1}\,s^{-1}},$$
$$k_{10} = 1\times10^9\ \mathrm{M^{-1}\,s^{-1}},$$
$$k_8 = 6\times10^7\ \mathrm{M^{-1}\,s^{-1}},$$
$$k_{13} = 1\times10^7\ \mathrm{M^{-1}\,s^{-1}},$$
$$k_{17} = k_{12} = k_3 = 1.0\ \mathrm{s^{-1}},$$
$$k_2 = 1.1626\ \mathrm{s^{-1}},$$
$$k_{16} = 1\times10^{-5}\ \mathrm{M\,s^{-1}},$$
$$E_t = 18.499\ \mu\mathrm{M}.$$

Table III gives the computed steady states for all species. With the initial conditions given in Fig. 6, we discover that there is a damped oscillatory approach to the steady state designated as SSIII in Table III.

Experimentally, Yamazaki *et al.*[19] first observed damped oscillations 20 years ago in a system with continuous supply of oxygen. It was also observed[19,20] that the oscillations in oxygen and compound III are synchronized. The present model reproduces this synchronized oscillations as shown in Fig. 6.

TABLE III. Computed steady state concentrations of all species in the bistable model for the peroxidase–oxidase reaction. (Parameter values given in the text.)

Species	Concentrations (10^{-7} M)		
	SSI	SSII	SSIII
A	83.2000	19.9895	1.0799
B	2.9263	2.0658	0.9925
C	8.5631	4.2677	0.9851
F	3.3044	4.6171	9.1532
W	0.1029	0.2135	0.9122
X	83.1719	82.0427	78.1411
Y	96.6956	95.3829	90.8468
Z	5.0196	7.3509	15.0899

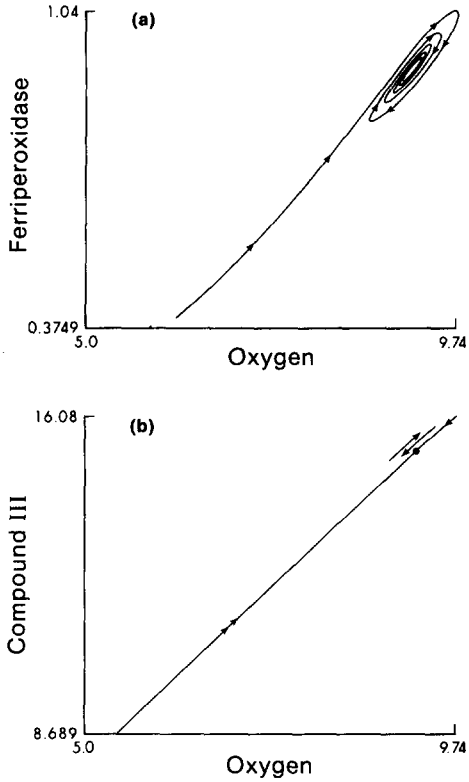

FIG. 6. Damped oscillatory approach to the steady state designated as SSIII in Table III. The damped oscillations in compound III and oxygen are synchronous as shown by the straight trajectory on the phase plot in (b). The parameter values used are given in the text. Initial conditions: $A(0) = 8.5$, $B(0) = 1.5$, $C(0) = 2.0$, $F(0) = 5.0$, $W(0) = 0.49$, $X(0) = 80.8$, $Y(0) = 95.0$, and $Z(0) = 8.7$ (units of 10^{-7} M).

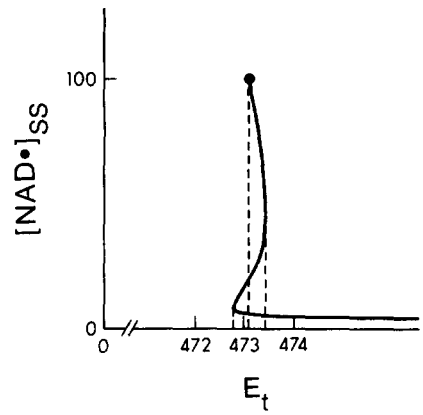

FIG. 7. Steady state bifurcation diagram for NAD· radical with the total enzyme concentration E_t as the bifurcation parameter. The network involved is the bistable model for the peroxidase–oxidase reaction shown in Fig. 4. The steady states of all the other species involved are expressible in terms of $[NAD^{\bullet}]_{ss}$ (see the text). The steady state curve terminates at a point corresponding to the vanishing of the enzyme species W and Z. [See also condition (5.4) in the text.] The parameters used are $k_{17} = 1.0\ s^{-1}$, $k_1 = k_{10} = 10^7\ M^{-1}\ s^{-1}$, $k_{11} = 10^8\ M^{-1}\ s^{-1}$, $k_{12} = 10^{-3}\ s^{-1}$, $k_2 = 0.6\ s^{-1}$, $k_3 = 0.3257\ s^{-1}$, $k_8 = 2.4\times10^7\ M^{-1}\ s^{-1}$, $k_{13} = 10^5\ M^{-1}\ s^{-1}$, and $k_{16} = 10^{-5}\ M\ s^{-1}$.

Figure 7 shows the steady state concentration of NAD· as a function of the total enzyme concentration (E_t) for the parameter values given in the figure. The curve terminates at a point which corresponds to the absence of the enzyme species W (ferriperoxidase) and Z (compound III). With the extinction of these species, the inhibition pathway is suppressed and the concentration of NAD· can increase without bound [primarily due to reactions R_{12}, R_2, and R_3 (see Table II)]. This is indeed the case in the region to the left of the terminal point in Fig. 7. There is a narrow region where two positive steady states can coexist for the same E_t value. The lower steady state is stable to small perturbations but the higher one is unstable and even the slightest increase in the concentration of NAD· above this steady state will lead to explosion. And to the left of this 2 steady state region, explosion of NAD· always occurs and no steady states are possible. Finally, a narrow range of E_t values to the right of the terminal point gives three steady states and the system is bistable.

C. Simulation of closed system kinetics

Attempts to fit some models to experimental data in a closed system have been performed by Yokota and Yamazaki[8] and Fed'kina *et al.*[9] In this section, we show that our model is also capable of accounting for several of the observed characteristic features of the closed system kinetics particularly that of compound III.

To simulate a closed system, we let $k_{16} = k_{17} = 0$. Note that besides the nonzero initial concentrations of oxygen and enzyme (W), either O_2^- or H_2O_2 must initially be present. Hydrogen peroxide is known to be produced by the autooxidation of NADH as represented by the following reaction:

$$NADH + O_2 + H^+ \rightarrow NAD^+ + H_2O_2.$$

This reaction is slow and can be ignored after the reaction system has started. It is mentioned here to justify the nonzero concentration of H_2O_2 initially. Figure 8 shows some concentration-time plots of oxygen and compound III. The parameter values are exactly those used by Yokota and Yamazaki[8] in their simulation except for the termination reaction (R_{13}) (see Table II) missing in their model, whose rate constant was assigned the value of $10^4\ M^{-1}\ s^{-1}$. Compound III kinetics involves the following phases likewise observed in experiments[8,9]: rapid increase, "steady state" and fast termination. There is no pronounced initial burst because of the low initial concentration of H_2O_2 which is consistent with experiment.[9] We also observed that the duration of the induction time (see oxygen concentration vs time plot) is independent of the initial oxygen concentration. During the steady state phase of compound III kinetics, a steady rate of oxygen consumption occurs.

To show explicitly that there is an inhibition of the catalyzed reaction by oxygen, we determine from the oxygen concentration vs time plots the steady state rates v_{st} [see Fig. 8(a)] of oxygen consumption for a given initial oxygen concentration. The result is given in Fig. 9, curve (a).

There is one maximum in the curve which is one characteristic of substrate inhibition of an enzyme reaction. However, as was also observed experimentally by Degn, Olsen, and Perram,[1] the rate does not fall off to zero at increasing oxygen concentrations as does the rate in the classical substrate inhibition model.

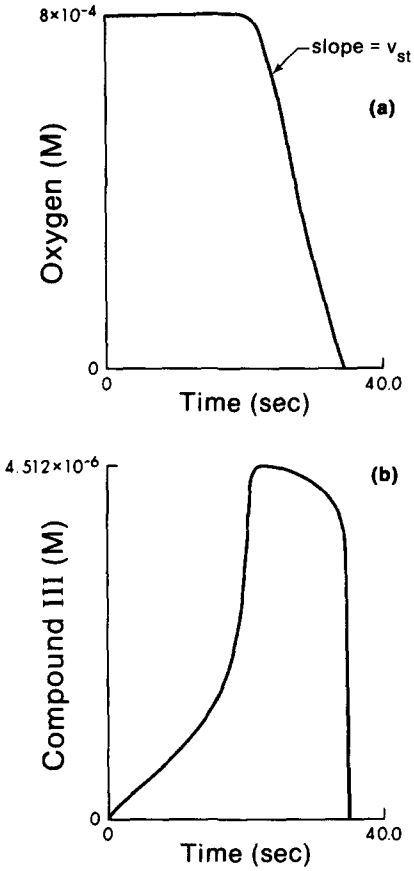

FIG. 8. A closed system is simulated by letting $k_{16} = k_{17} = 0$ with the following initial species concentrations: $[O_2]_0 = 8\times10^{-4}$, $[H_2O_2]_0 = 10^{-8}$, $[NAD^{\cdot}]_0 = 10^{-8}$, $[O_2^{-}]_0 = 10^{-8}$, $[NADH]_0 = 10^{-3}$, $[Per^{3+}]_0 = 6.75\times10^{-6}$, $[Co\ I]_0 = 10^{-8}$, $[Co\ II]_0 = 3\times10^{-8}$, and $[Co\ III]_0 = 10^{-8}$. (a) Time course of oxygen concentration showing an induction period and a steady rate (v_{st}) of oxygen consumption. (b) Kinetics of compound III showing a rapid increase in its concentration during the oxygen induction period, a near steady state phase, and a rapid termination phase. The parameters used are $k_{11} = 2\times10^{9}$, $k_{12} = 5.9\times10^{3}$, $k_1 = 1.8\times10^{7}$, $k_2 = 5.4\times10^{3}$, $k_3 = 8\times10^{2}$, $k_{10} = 1.9\times10^{6}$, $k_8 = 1.3\times10^{8}$, and $k_{13} = 10^{4}$.

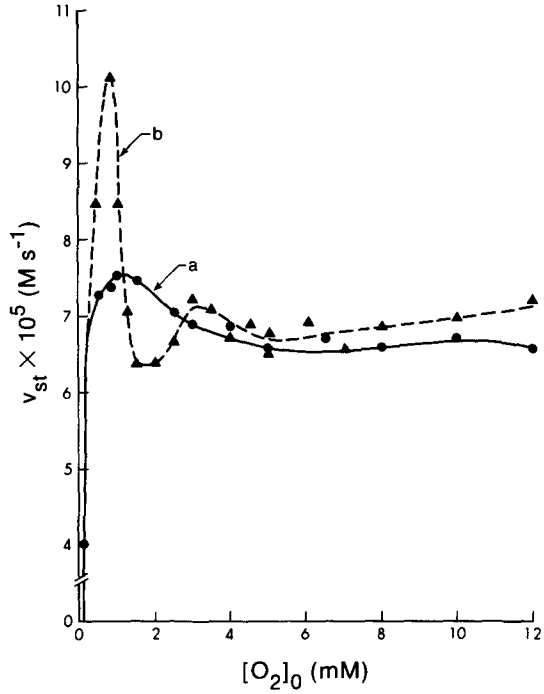

FIG. 9. Steady rate of oxygen consumption v_{st} as a function of initial oxygen concentration for the peroxidase–oxidase reaction in a closed system. Curve (a): Simulated experiments exemplified by Fig. 8(a) were repeated for various initial oxygen concentrations and the corresponding v_{st} measured. The bistable model given in Fig. 4 was used with $k_{16} = k_{17} = 0$ and the same parameters used in Fig. 8. Curve (b): Reaction R_7 ($k_7 = 10^2$) (of Table II) is included to the model and similar simulated experiments were done.

The experimental results[1] showed that the peak of the curve is relatively higher than that shown by our model in Fig. 9, curve (a). This is due to the deletion of other reactions which have a quantitative effect on the simulations. For instance, when we add the slow reaction R_7 (Table II) to our model we find a higher peak in the curve [see curve (b)]. (The rate constant used for this reaction was 100 M^{-1} s^{-1} as given in Ref. 20.) This result can be explained by the higher degree of autocalysis with respect to the NAD radical introduced by the extreme current E^{14} which will directly increase the rate of oxygen consumption via R_{11} (Table II).

VI. SUMMARY AND CONCLUSIONS

A systematic way of determining the dominant steady state reaction pathways or extreme currents under bistable conditions had been presented and applied towards the modeling of the bistability observed in the peroxidase–oxidase reaction. The two essential ingredients in our approach are: (a) the structure of the current polytope Π_v showing how the extreme currents are coupled to each other, and (b) the necessary test given by the vanishing of $\alpha_d(\mathbf{h},\mathbf{j})$ for the existence of multiple steady states. Our modeling approach also, in effect, gave a convenient method for testing whether or not a given complex mechanism is capable of bistability or, in general, multiple steady states by looking at the two-dimensional faces of Π_v.

It was pointed out that for bistability or three steady states, there must be at least three extreme currents comprising a model network. Our model contains the minimum number of extreme currents found from a list of elementary steps involved in the PO reaction. The analysis of this model in Sec. V showed that it was able to reproduce several experimentally observed features of the reaction like damped oscillations which occurred simultaneously with bistability, synchronous oscillation between oxygen and compound III, the characteristic phases of the kinetics in a closed system, and explicitly demonstrated the substrate-inhibition mechanism causing the bistability.

We also saw that three basic elements found both in the classical substrate-inhibition mechanism and in our model are sufficient to cause bistability, namely, (i) reversible flux of a substrate, (ii) a catalytic cycle, and (iii) a substrate-inhibition pathway (or cycle) coupled to the catalytic cycle.

No attempt has yet been made to show whether or not our model may also exhibit sustained oscillations or chaos for some parameter values. An extension of our modeling approach to include these dynamical features is planned.

[1]H. Degn, L. Olsen, and J. Perram, Ann. N. Y. Acad. Sci. **316**, 623 (1979).
[2]H. Degn and D. Mayer, Biochim. Biophys. Acta **180**, 291 (1969).
[3]A. Lotka, J. Phys. Chem. **14**, 271 (1910).
[4]L. F. Olsen and H. Degn, Biochim. Biophys. Acta **523**, 321 (1978).
[5]L. F. Olsen, Phys. Lett. A **94**, 454 (1983).
[6]L. F. Olsen, in *Stochastic Phenomena and Chaotic Behavior in Complex Systems*, edited by P. Schuster (Springer, Berlin, 1984), p. 116.
[7]L. J. Aarons and B. F. Gray, Chem. Soc. Rev. **5**, 359 (1976).
[8]K. Yokota and I. Yamazaki, Biochemistry **16**, 1913 (1977).
[9]V. R. Fed'kina, F. I. Ataullakhanov, T. V. Bronnikova, and N. K. Balabaev, Stud. Biophys. **72**, 195 (1978).
[10]B. L. Clarke, Adv. Chem. Phys. **43**, 1 (1980).
[11]B. L. Clarke, J. Chem. Phys. **75**, 4970 (1981).
[12]B. von Hohenbalken, Math. Program. **15**, 1 (1978).
[13]B. D. Aguda, Ph. D thesis, University of Alberta, 1986.
[14]I. Yamazaki and L. Piette, Biochim. Biophys. Acta **77**, 47 (1963).
[15]I. Yamazaki and K. Yokota, Mol. Cell. Biochem. **2**, 39 (1973).
[16]H. Degn, Biochim. Biophys. Acta **180**, 271 (1969).
[17]K. Yokota and I. Yamazaki, Biochim. Biophys. Acta **105**, 301 (1965).
[18]V. R. Fed'kina, F. I. Ataullakhanov, and T. I. Bronnikova, Biophys. Chem. **19**, 259 (1984).
[19]I. Yamazaki, K. Yokota, and R. Nakajima, Biochem. Biophys. Res. Commun. **21**, 582 (1965).
[20]I. Yamazaki and K. Yokota, Biochim. Biophys. Acta **132**, 310 (1967).